Bioorganic Chemistry 92 (2019) 103216

Contents lists available at ScienceDirect

Bioorganic Chemistry

journal homepage: www.elsevier.com/locate/bioorg

Synthesis, *in-vitro* cholinesterase inhibition, *in-vivo* anticonvulsant activity and *in-silico* exploration of *N*-(4-methylpyridin-2-yl)thiophene-2-carboxamide analogs

Gulraiz Ahmad[a], Nasir Rasool[a,*], Komal Rizwan[a,b], Imran Imran[c], Ameer Fawad Zahoor[a], Muhammad Zubair[a], Abdul Sadiq[d], Umer Rashid[e,**]

[a] Department of Chemistry, Government College University, Faisalabad 38000, Pakistan
[b] Department of Chemistry, Government College Women University, Faisalabad 38000, Pakistan
[c] Department of Pharmacology, Faculty of Pharmacy, Bahauddin Zakariya University 60800 Multan, Pakistan
[d] Department of Pharmacy, University of Malakand, Chakdara 18000 Dir (L), Pakistan
[e] Department of Chemistry, COMSATS University Islamabad, Abbottabad Campus, 22060, Pakistan

ARTICLE INFO

Keywords:
Carboxamides
Anticonvulsive
Cholinesterases
In vivo
Pentylenetetrazole
Suzuki coupling

ABSTRACT

In our current research, a diverse effect of acetylcholinesterase inhibitors was studied on BALB-C mice by using pentylenetetrazole (PTZ) seizure model. A series of carboxamide analogs (**4a–4i**) have been synthesized *via* Suzuki coupling reaction in moderate to good yields (35–84%). To study the efficacy of the synthesized compounds against AD, *in-vitro* inhibition of acetylcholinesterase (AChE) and butyrylcholinesterase (BChE) was performed. A number of compounds showed inhibition in low micromolar range. Subsequently, these compounds were evaluated for anticonvulsive effects in BALB-C mice by using pentylenetetrazole (PTZ) seizure model. The compound **4e** displayed potential anticonvulsive effect and displayed 50% and 80% protection from mortality at the dose of 10 mg/kg, and 30 mg/kg respectively. The compound **4h** showed some protection (33%) from mortality at 10 mg/kg and was not further explored based on non-significant delay in onset of myoclonic seizures. While, other compounds from the series did not show any anticonvulsive activity. To rationalize the observed biological activity, we performed docking studies against AChE and BChE targets. To explore the rationale of the mechanism of *in-vivo* anticonvulsant activity, docking studies were performed on GABAergic receptors. Moreover, in order to establish a relationship between physiochemical data of the synthesized compounds and their *in-vivo* performance, we employed *in-silico* pharmacokinetic predictions. Our *in-silico* predictions suggest that the plasma protein binding, low to moderate blood brain barrier penetration and low solubility are the main attributes of low *in-vivo* performance.

1. Introduction

Epilepsy is a common, serious and chronic neurological disease due to brief disturbances in electrical functions of the brain and associated with co-morbidities and social discrimination. Epilepsy affects people of all age and is categorized into many types based on the involvement of brain lobes. The characteristic feature of epilepsy is recurrent seizures and it can differentiate from short and nearly unnoticeable to long periods of vigorous convulsions [1–3]. Reports of world health organization (WHO) revealed that more than 65 million people are suffering from epilepsy worldwide, out of them 80% are living in developing countries with serious compromising to the quality of life [4]. During the past years, several new anti-epileptic drugs (AEDs) have been approved. However, these new generation drugs also cause some central nervous system disorders [5–7]. Therefore, window remained open to find new sources of epileptic drugs.

Alzheimer's disease (AD) is a neurodegenerative brain disorder and most common form of dementia, in which an affected person may loss memory, shows decline in language, and irreversible emotional or mental impairments. Various pathological hypotheses have been put forth to explain the onset and progression of AD. These all hypothesis are based on the biochemical phenomenon found to be happening in the brains of AD patients. Among all these, the cholinergic hypothesis is widely accepted and inhibition of both cholinesterases i.e

* Corresponding author.
** Corresponding author.
E-mail addresses: nasirrasool@gcuf.edu.pk (N. Rasool), umerrashid@cuiatd.edu.pk (U. Rashid).

https://doi.org/10.1016/j.bioorg.2019.103216
Received 21 March 2019; Received in revised form 20 August 2019; Accepted 21 August 2019
Available online 23 August 2019
0045-2068/

acetylcholinesterase (AChE) and butyrylcholinesterase (BChE) is found to be the only effective therapeutic approach for AD up till now [8].

Alzheimer's disease (AD) and epilepsy are frequently associated with neurological disorders (NDs). In the last decade, there are growing evidences that linked seizure-like activity occurring in the brain of AD patients [9,10]. It has been reported that approximately 10–22% of patients with AD are susceptible to unprovoked seizures. Although highest occurrence of epilepsy is associated in a range of ages of AD patients. However, several retrospective studies have shown that seizures occur in elderly patients more frequently [4,11]. Raudino reviewed Medline literature until July 2016 and revealed that AD and epilepsy are interlinked, and both can appear simultaneously in the same patient [12]. A study by Vossel et al., on 54 patients found the time period of onset of cognitive impairment in patients with and without epilepsy [13].

Numerous studies reported the ameliorating effect of ACH inhibitors in the epileptic patients with the significant nootropic effect [11]. Jeong et al., evaluated the diverse effect of AChE inhibitor donepezil on brain injury after pilocarpine-induced seizures [11,14]. Mishra and Goel suggested in a preclinical adjuvant tacrine (anticholinesterase drug) therapy for the Management of Epilepsy-Induced Memory Deficit [15]. Memantine, a glutamate NMDA receptor antagonist, is commonly prescribed drug in AD patients. Some studies on animal models of epilepsy revealed that memantine has shown anticonvulsant properties [16,17]. On the other hand, Sanchez et al., it was demonstrated that use of new generation anti-epileptic drug (AEDs) i.e. Levetiracetam (LEV, Fig. 1**b**) which has relatively less adverse effect profile can ameliorate cognitive, and behavioral dysfunctions in experimental animal models [11,18–21]. Similarly, a study conducted by Nygaard et al demonstrated that another potent epilepsy drug brivaracetam (Fig. 1**c**) is effective in treatment of memory impairment in AD mice [22]. The neurologists anticipated that in future these two epilepsy drugs will be part of therapeutic arsenal against AD.

Our ongoing research focuses on design and synthesis of pharmacologically active compounds. Our research group is involved in the synthesis of diverse scaffolds as inhibitors of cholinesterase [23,24]. We have also previously reported synthesis of compounds using Suzuki cross-coupling reaction [25–29]. In current study, we selected N-(4-methylpyridin-2-yl)thiophene-2-carboxamide core for further chemical derivatization. Some coumarin-3-carboxamide derivatives linked to *N*-benzylpiperidine scaffold were reported by Asadipour et al. as potent AChE inhibitors [30]. The main aim of current study was to identify a drug or molecule which at one hand can target the excitability of the brain to exert its calm effect and on other hand proportionally decrease excitotoxicity to prevent the progression of Alzheimer disease. To study the effect of the compounds against Alzheimer's disease, we planned to perform *in-vitro* assays on acetylcholinesterase and butyrylcholinesterase. Furthermore, the study of the diverse effect of these acetylcholinesterase inhibitors was planned on BALB-C mice model. Herein, we report the synthesis of diverse compounds that can act as polyvalent compounds and are able to target simultaneously two neurological disorders i.e. Alzheimer disease and epilepsy.

2. Results and discussion

2.1. Design rational

The idea was to design the inhibitors that can target simultaneously two neurological disorders i.e. AChE and epilepsy. We decided to introduce thiophene carboxamide core to design multitarget compounds. Carbamazepine (Fig. 1**a**) is a common carboxamide based anticonvulsive drug and it is sold in market with name Tegretol. It is used for treatments of seizures, but it also has many side effects [31]. Like carbamazepine, levetiracetam and brivaracetam are carboxamide containing antiepileptic drugs (Fig. 1**b–c**). Based on the insights gained from the active site gorge of the AChE, which contains fourteen aromatic amino acids [32], we have proceeded to design a molecular framework that contain hydrophobic rings on each side of thiophene carboxamide core (antiepileptic drugs pharmacophore). Our design strategy involved incorporating the aryl rings on the both sides of the linker (Fig. 1**d**). We were in opinion that these aryl rings may form π-π stacking interactions with aromatic residues of distinctive functional activities (Trp84 and Trp279 of *Tc*AChE numbering). Furthermore, nitrogen atom of pyridine ring may involve in hydrogen bond interactions.

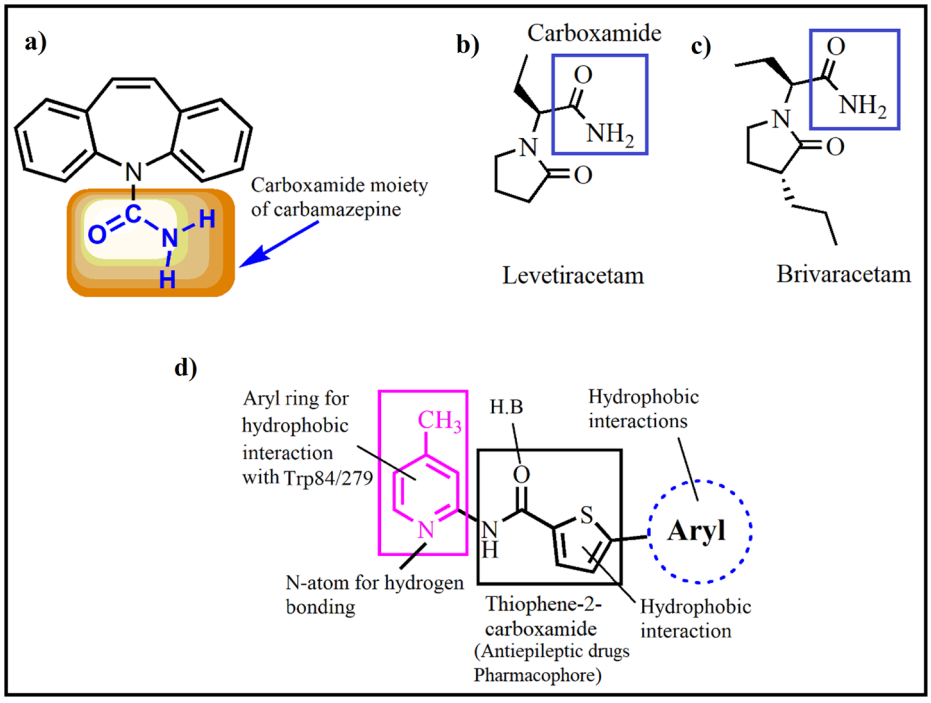

Fig. 1. Rationale of the designed strategy.

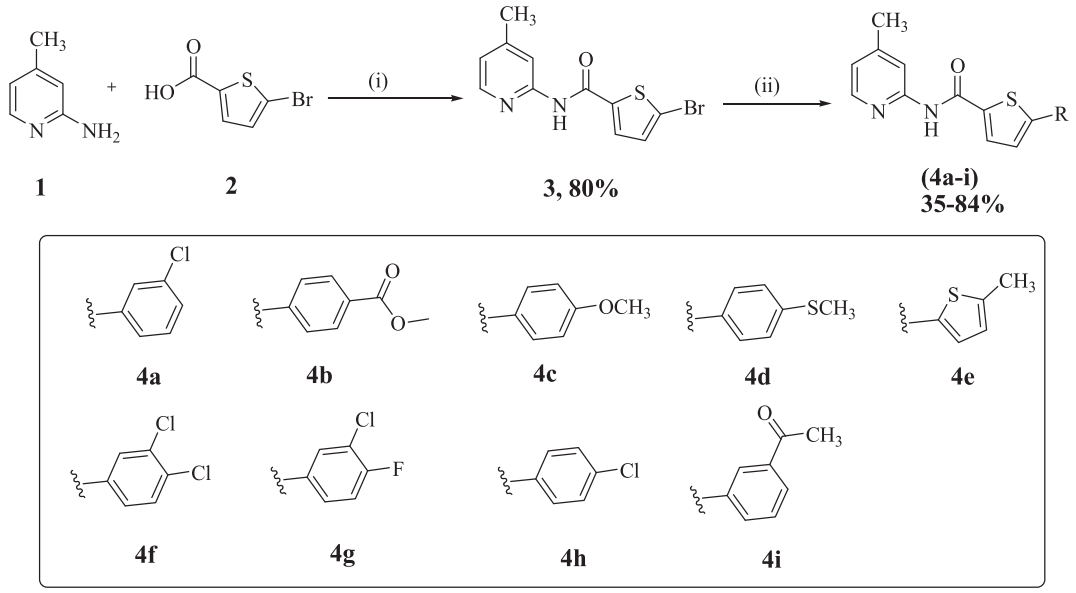

Scheme 1. Protocol for the synthesis of intermediate compound 5-bromo-N-(4-methylpyridin-2-yl)thiophene-2-carboxamide **(3)** and arylated carboxamide analogues **(4a–i).** Conditions: *i*, **1** (14.48 mmol, 1 eq, 3.0 g), **2**, (14.48 mmol, 1 eq, 1.567 g), $TiCl_4$ (43.5 mmol, 3.0 eq, 4.78 mL), pyridine (150 mL), 2 h, 85 °C; *ii*, **3**, (1 eq, 0.673 mmol, 0.2 g), $Pd(PPh_3)_4$ (7 mol%, 0.0544 g), aryl/het-aryl boronic acid/ester (1.1 eq, 0.740 mmol), K_3PO_4 (2 eq, 1.35 mmol, 0.284 g), 1,4-dioxane/H_2O (4:1), 20–25 h, 90 °C under nitrogen atmosphere.

2.2. Chemistry

The synthetic route to the targeted compounds is outlined in Scheme 1. The intermediate compound 5-Bromo-N-(4-methylpyridin-2-yl)thiophene-2-carboxamide **(3)** was synthesized by reacting 2-amino-4-methylpyridine **(1)** and 5-bromothiophene-2-carboxylic acid **(2)** in the presence of titanium tetrachloride ($TiCl_4$). In the second step, the intermediate compound **(3)** was coupled with aryl/het-aryl boronic acids/esters under Suzuki coupling reaction conditions, using Pd $(PPh_3)_4$ as catalyst that eventually led to the synthesis of various carboxamide derivatives **(4a-i)** in moderate to good yields (35–84%) (Table 1, Scheme 1). For the substrates incorporating methoxy **(4c),** 3-chloro **(4a),** 3,4-dichloro **(4f)**, 4-chloro **(4h)** and 3-chloro-4- fluoro **(4g)** provided high yields. The thiomethyl derivative **(4d)** also provided a good yield. The substrate containing 4-carboxymethyl **(4b)** group afforded low yield, this may be due to steric hindrance. Different electron donating and withdrawing groups were successfully tolerated under reaction conditions. To generalize this method, under the same reaction conditions, heteroaryl boronic ester (5-methylthiophene-2-boronic acid pinacol ester) was coupled with **(3)** and desired product **(4i)** was obtained in high yield (80%). Of note, methyl substituent on the het-aryl boronic ester was also well tolerated.

Table 1
In vitro AChE and BChE inhibitory activity of the synthesized compounds.

Compound	IC_{50} (μM ± SEM)[a]		SI[b]
	eeAChE	eqBChE	
4a	19.4 ± 0.91	8.45 ± 0.10	0.4
4b	**3.08 ± 0.34**[c]	**1.65 ± 0.03**	0.5
4c	**6.92 ± 0.41**	6.59 ± 0.13	0.9
4d	11.2 ± 0.29	12.9 ± 1.03	1.1
4e	17.4 ± 1.01	19.3 ± 1.11	1.1
4f	8.31 ± 0.31	35.6 ± 1.19	4.3
4g	13.4 ± 0.24	59.7 ± 1.10	4.4
4h	21.4 ± 0.31	30.8 ± 1.28	1.5
4i	**4.51 ± 0.39**	23.6 ± 1.31	5.2
Galantamine	4.2 ± 0.11	15.8 ± 0.38	3.7
Donepezil	0.055 ± 0.01	6.0 ± 0.27	109.0

[a] SEM = Standard Error of Mean.
[b] Selectivity Index = IC_{50} of BChE/IC50 of AChE.
[c] Bold values are for compounds showed good inhibition

2.3. Pharmacology

2.3.1. In-vitro cholinesterases (ChEs) inhibition studies

We evaluated our synthesized compounds against acetylcholinesterase (*ee*AChE) and butyrylcholinesterase (*eq*BChE) by using Ellman's method. Galantamine and donepezil was used as standard drug. The *in-vitro* activity results in terms of IC_{50} value are enlisted in Table 1. The AChE selectivity was determined by analyzing selectivity index (SI = IC_{50} of BChE/IC_{50} of AChE). The data in Table 1 showed that all the synthesized compounds exhibited moderate to good activity. For compounds **4a–c**, low SI value showed the reduced selectivity for AChE inhibition. Compound **4a** with SI of 0.4 showed good BChE inhibition (IC_{50} = 8.45 μM). However, it failed to show good eeAChE inhibition 19.4 ± 0.91 μM). Although, compound **4b** with IC_{50} value of 3.08 ± 0.34 μM emerged as good inhibitor of eeAChE, but, the same compound showed high selectivity for BChE (IC_{50} = 1.65 ± 0.03 μM, SI = 0.5). Compound **4i** with IC_{50} value of 4.51 ± 0.39 μM emerged as another good and selective inhibitor of eeAChE. However, it showed poor BChE inhibition (IC_{50} = 23.6 ± 1.31 μM, SI = 5.2). All the other compounds showed moderate activity.

2.3.2. Anticonvulsive studies

In this study, the acute PTZ seizure model was used for the initial anticonvulsive screening of synthesized **4a–4i** compounds and data are shown in Table 2. The control epileptic group after having PTZ typically showed the development of first myoclonic jerks within 70.6 ± 6.3 s and generalized clonic convulsions at 156.6 ± 18.5 s. There was 100% mortality due to hyperexcitability and convulsions within 3–4 min of administration of chemoconvulsant. The total duration of convulsions in PTZ control group lasted not more than 3 min. The mice treated with diazepam (5 mg/kg) plus PTZ showed 100% protection from convulsions and mortality ($P < 0.001$ compared to control; n = 6–8). Among the tested compounds, only **4e** displayed anticonvulsive potential at the dose of 10 mg/kg with significant delay in the development of first myoclonic jerks (172.3 ± 10.5 s compared to control; $P < 0.01$ vs

Table 2
Anticonvulsive potential of synthesized compounds **(4a–i)** in acute pentylenetetrazole (PTZ 90 mg/kg) induced seizures in experimental mice model.

Group	Dose	Latency to onset of Tonic seizures (Sec)	Latency to onset of Clonic seizures (Sec)	%age of animals convulsed	%age of animals protected from seizures/Mortality
Control (PTZ)	90 mg/kg	70.66 ± 6.33	156.67 ± 18.56	100%	0%
Standard (Diazepam)	(5 mg/kg)	No Seizure	No Seizure	0%	100%
4a	10 mg/kg	102 ± 18.05	201 ± 41.93	100%	0%
4b	10 mg/kg	43.33 ± 14.81	148.67 ± 94.27	100%	0%
4c	10 mg/kg	63.00 ± 31.53	353.33 ± 6.93*	100%	0%
4d	10 mg/kg	68.33 ± 17.47	231.67 ± 62.43	100%	0%
4e	10 mg/kg	172.33 ± 10.53**	181.33 ± 22.52^{ns}	50%	50%
	30 mg/kg	388.00 ± 47.95***	723.33 ± 25.22***	20.0%	80.0%
4f	10 mg/kg	104.33 ± 64.59	120.00 ± 34.18	100%	0%
4g	10 mg/kg	45.00 ± 8.73	68.67 ± 14.49	100%	0%
4h	10 mg/kg	99.67 ± 31.75	472.5 ± 127.5	66.67%	33.33%

Data values are represented as mean ± SEM (n = 6–8) which are analyzed by using one-way ANOVA followed by Dunnett's test. *P < 0.05; **P < 0.01; ***P < 0.001; ns = not significant (*vs* control group, PTZ 90 mg/kg).

Control) but not significant latency observed with generalized seizures (191.3 ± 22.5 s compared to control, P > 0.05, ns vs control). However, the compound **4e** displayed 50% protection from mortality, which is the good sign of further exploration and therefore **4e** was further explored at the dose of 30 mg/kg. The observed results in Table 2**,** indicated that **4e** displayed potential anticonvulsive effect and displayed 50% and 80% protection from mortality at the dose of 10 mg/kg, and 30 mg/kg respectively. Compound **4 h** showed some protection (33%) from mortality at 10 mg/kg and was not further explored based on non-significant delay in onset of myoclonic seizures (P > 0.05). In experimental studies with animals, we did not observe any sign of severe illness with the exception of seizures.

Carbamazepine-related antiepileptic drugs are believed to possess multiple proposed antiseizure mechanisms such as blockage of central sodium channels, potentiation of GABA neurotransmission and down-regulation of glutamate [31]. In our experimental settings, we used acute PTZ model which induces convulsion in rodents by antagonizing the GABAergic transmission and therefore mimicking the glutamate pathways resulting in excitation. Compound **4e** at the dose of 30 mg/kg demonstrated significant anticonvulsive effect which might be due to the high affinity with GABA-A receptor which in result increases the hyperpolarization of neuronal membranes and therefore decreased the hyperexcitability. We employed the diazepam as a standard drug sharing the similar mechanism of action.

2.4. In-silico studies

Docking studies on Cholinesterases (Acetylcholinesterase and butyrylcholinesterase) were carried out using Molecular Operating Environment (MOE 2016.0208) software package. We have also performed a massive *in silico* exploration of possible mechanism of the antiepileptic activity. Here, we extended our study to explore the antiepileptic activity by using in-silico tools. It is difficult to assume the biomolecular target for the *in-vivo* antiepileptic activity. However, we are in opinion that the reference drug used in current study will provide some insight toward mechanism. To study the outcomes of *in- vivo* results, the modulation study of the synthesized compounds was explored by molecular docking studies using MOE 2016.0208. In this *in vivo* study, diazepam was used as reference drug. Diazepam is a well-known GABA-A receptor agonist. Hence, docking studies on different GABA receptors were carried out. First, docking studies were carried out on human GABA-A receptor complexed with benzamidine as native ligand. To rationalize these results, we further selected a pentameric ligand-gated ion-channel from *Erwinia chrysanthemi*. The GABA-A receptors is composed of GABA (activator) binding site and an allosteric site bound with flurazepam (Modulator). Additionally, we also chose γ-aminobutyric acid aminotransferase (GABA-AT) as molecular target. The inhibition of GABA-AT raises brain GABA level and thus terminates seizures.

Furthermore, we initiated in silico pharmacokinetics prediction of the compounds to establish *in vivo-in silico* relationship. The goal of this study is to predict the *in-vivo* pharmacokinetic studies of our newly synthesized compounds based on their virtual structure and their derived parameters. A number of molecular descriptors were computed as indicator of pharmacokinetic properties. The molecular descriptors related to bioavailability, plasma protein binding (PPB) and blood brain barrier (BBB) penetration were computed. The parameters for oral absorption assessed are permeability (logPer), solubility (Sw) of the synthesized compounds and compliance with the Lipinski Rule of Five (Ro5). The Lipinski parameters determined are size of the molecule, their ability to form hydrogen bonds, lipophilicity, topological surface area (TPSA) and molecular flexibility were determined. Distribution coefficient (log D) of all compounds was predicted in the various environments of alimentary canal. Plasma protein binding (PPB) of drugs reduces their bioavailability. Hence, only a less bound drug is responsible for any pharmacological activity. PPB of the most active compound were also predicted.

2.4.1. Docking studies on cholinesterases

Docking studies were carried out *via* MOE docking software. The three-dimensional (3-D) crystal structure of *Torpedo californica* (*Tc*AChE) with donepezil as native ligand was retrieved from Protein Data Bank (PDB accession code 1EVE) [33]. While, 3-D crystal structure of BChE was obtained with PDB accession code 1P0I [34]. Before docking of synthesized compounds, the re-dock method was used to validate the docking procedure. The computed root means square deviation (RMSD) computed for re-docking of native donepezil into the AChE biding site is 0.993 Å which is within the acceptable criteria (< 2 Å). The binding pocket of *Tc*AChE consists of residues present in peripheral anionic site (PAS), catalytic active site (CAS), catalytic triad, acyl pocket and oxyanion hole [32,35,36]. Docking results of the synthesized compounds revealed that all the compounds occupy the space in the *Tc*AChE active site like the native donepezil (Fig. 2**a**). The binding orientation of most active compound **4b** superimposed on native donepezil into the AChE active site is shown in Fig. 2**a**. The 3-D interaction plot of donepezil (standard drug) showed π-π stacking interaction with Trp279 as well as with Trp84 (Fig. 2**b**). A π−H bond is also observed between piperidine ring proton and Phe330. The 3-D interaction plot shown in Fig. 2**c** revealed that compound **4b** established a π-π stacking interaction with Trp279 *via* pyridine ring. Phe331 forms π-π stacking interaction with thiophene ring. While, Phe330 also established π-π stacking interaction with benzoate ring. Sulfur atom of thiophene ring was involved in π-sulfur type of interactions with Phe290. Trp84 was engaged in π-alkyl interactions (Fig. 2**c**).

For BChE, the docking pose of compound **4b** is shown in Fig. 2**d**. Trp82 is involved in a strong bifurcated π-π stacking interaction with

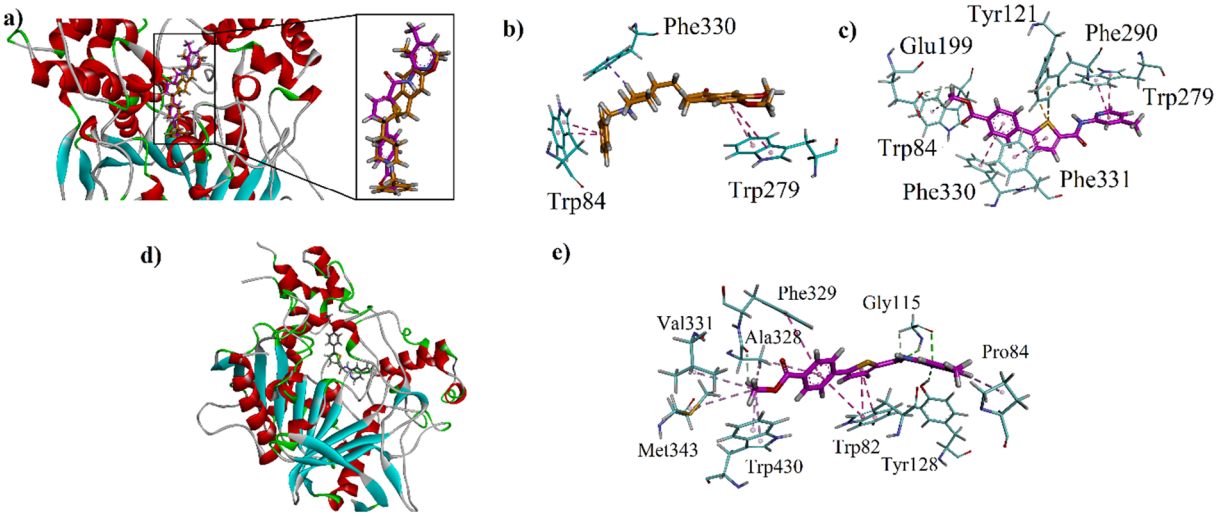

Fig. 2. (a) The overlaid ribbon diagram of synthesized compound **4b** and native ligand donepezil into the binding site of AChE (PDB 1EVE). **(b)** Close-up 3-D interaction plot of standard drug donepezil into the binding site of AChE (PDB 1EVE) **(c)** Close-up 3-D interaction plot of compound **4b** into the binding site of AChE. **(d)** Ribbon diagram of synthesized compound **4b** into the binding site of BChE (PDB 1P0I). (**e**) Close-up 3-D interaction plot of compound **4b** into the binding site of BChE (PDB 1P0I).

thiophene as well as benzoate ring. Phe329 also forms π-π stacking interaction with benzoate ring. Two hydrogen bond interactions (HBI) are also found between 4c and active site residues. Gly115 forms HBI with carbonyl oxygen of amide. While, another HBI was found between nitrogen atom of pyridine ring and Tyr121. A number of weak π-alkyl type of interactions were also found (Fig. 2**e**).

2.4.2. Docking studies on GABA-A receptors

To explore the mechanism of anticonvulsant activity, we performed docking studies on GABA-A receptor. For this purpose, we downloaded three-dimensional structure of human GABA-A receptor (PDB accession code = 4COF) complexed with benzamidine as native ligand [37]. Before docking of target compounds, algorithm was validated by the re-docking of the native ligand. The root mean square deviation (RMSD) was computed and was found within the threshold limit i.e. < 2.0 Å. For the investigation of binding orientations and interacting residues, we docked standard drug diazepam used for *in-vivo* studies. Furthermore, we also analyzed the binding pattern of methaqualone (a positive allosteric GABA-A receptor modulator) to confirm the docking accuracy. Three-dimensional interaction plot of these two reference drugs is shown in Fig. 3**a-b**. the key amino acid residues interact with these drugs are Tyr62, Gln64 and Met115. Inspection of the binding modes demonstrated that all synthesized compounds were bound to the active site of reference and native drugs. Ribbon diagram of docking orientation of all the synthesized compounds superimposed on diazepam, native ligand and methaqualone is shown in Fig. 3**c**.

Compound **4e** binding mode revealed a strong bifurcated interaction of Gln64 with carbonyl oxygen (1.95 Å) and pyridine nitrogen (2.51 Å) atom. Pyridine ring oriented itself in such a way to form a π-π stacking interaction with Tyr62. Sulfur atom of thiophene ring was involved in π-sulfur type of interactions with Tyr62 (Fig. 4**a**). Almost same type of interactions was also shown by compound **4 h** (Fig. 4**b**). However, **4 h** shows strong binding affinity (−6.0378 kcal/mol) compared to **4e** (−5.8145 kcal/mol).

Further for rationalizing results, we selected a pentameric ligand-gated ion-channel from Erwinia chrysanthemi (PDB accession code 2YOE). The GABA-A receptor is composed of GABA (activator) binding site and an allosteric site bound with flurazepam (Modulator, Fig. 5**a**). Before the docking simulation of synthesized compounds, standard drug diazepam was docked into the active site. Our docking study revealed that diazepam and the synthesized compounds are

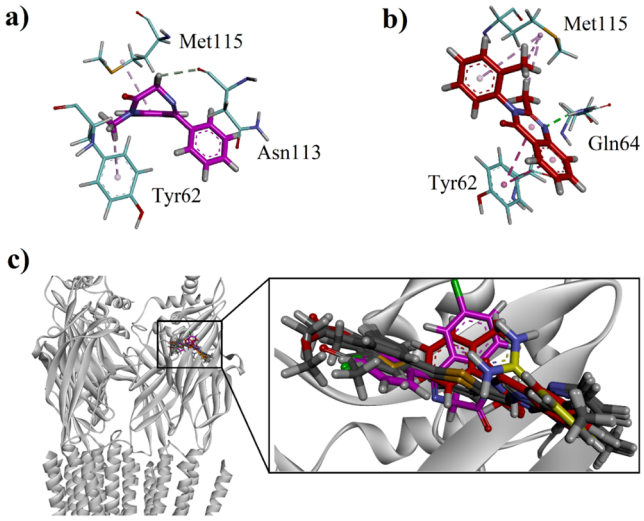

Fig. 3. (a–b) Close-up 3-D depiction (line-model) of reference drugs diazepam and methaqualone (stick-model) (**c**) The overlaid ribbon diagram of synthesized compounds, diazepam (pink), methaqualone (red) and native ligand (yellow) into the binding site of GABA-A receptor (PDB accession code = 4COF).

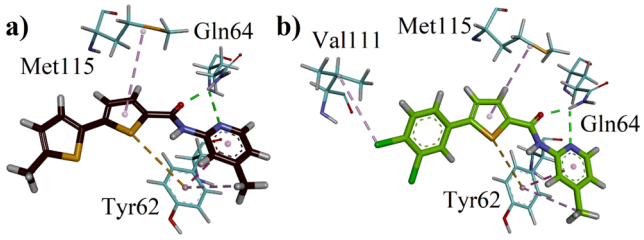

Fig. 4. (a–b) Close-up 3-D interaction plot of compound **4e (a)** and **4h (b).**

accommodated into the flurazepam allosteric site (Fig. 5**b**). The binding affinities of the synthesized compounds were all in range −7.2366 to −5.9831 kcal/mol.

We have also performed docking studies on gamma aminobutyric acid aminotransferase (GABA-AT) receptors. The docking results are presented in Supporting Information.

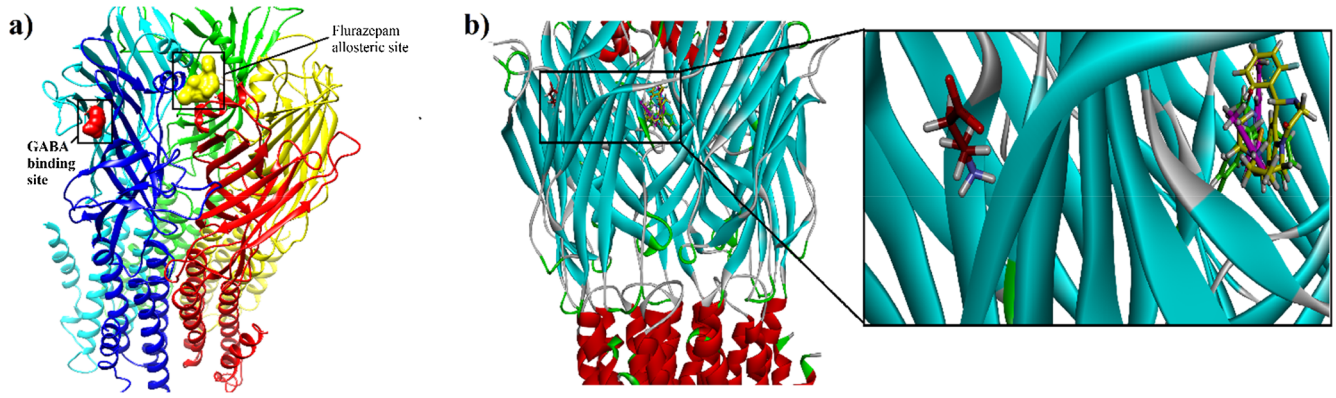

Fig. 5. (a) Three-dimensional (3-D) structure of pentameric ligand-gated ion-channel from Erwinia chrysanthemi (PDB accession code 2YOE) showing allosteric binding site (flurazepam site) and GABA binding site. (b) 3-D docking pose of the active compound 4e (pink) superposed on diazepam (green) into the binding site of 2YOE.

Table 3
In-silico parameters predicted to study the preliminary pharmacokinetics of the synthesized compounds.

Compd	PPB (%)	BBB Penetration		HIA	Water solubility (mg/L)	AMES Toxicity (Probability)	Carcinogen (Probability)
		PreADMET	BBB predictor				
4a	91.0	0.2	0.11	96.3	0.79	− (0.5460)	− (0.8365)
4b	92.5	0.02	0.09	96.8	0.99	− (0.6495)	− (0.8506)
4c	93.5	0.02	0.10	96.5	3.57	+ (0.6027)	− (0.9099)
4d	90.0	0.05	0.15	96.8	0.84	− (0.6077)	− (0.8902)
4e	89.0	0.13	0.11	97.5	**16.26**	− (0.6888)	− (0.8810)
4f	94.4	0.33	0.09	96.8	0.11	− (0.55657)	− (0.8353)
4g	92.0	0.16	0.10	96.4	0.38	− (0.5270)	− (0.8157)
4h	91.6	0.13	0.11	96.4	0.75	− (0.5460)	− (0.83650
4i	95.7	0.05	0.13	96.8	1.04	− (0.5835)	− (0.8292)
D	98.7	2.58	0.15	99.5	**6.17**	− (0.0.9133)	− (0.0.8312)

2.4.3. Preliminary in-silico pharmacokinetic studies

In order to establish a relationship between physiochemical data of the synthesized compounds and its *in vivo* performance, we employed *in-silico* pharmacokinetic parameters. In contrast to the *in-vitro* studies, the complex system of the whole body responds differently to the drug in the *in-vivo* experiments. There is chance of promising activity *in-vitro*, however, subsequent *in vivo* experiments may result in failure in terms of efficacy or safety parameters. Binding affinity data computed *via* docking simulations against GABA-A/GABA-AT receptors showed that these receptors are possible mechanism of action for the synthesized compounds. As the lack of drug activity is directly related with poor pharmacokinetic parameters, therefore, we proceeded towards calculation of pharmacological and pharmacokinetic parameters.

In order to cross different physiological barriers, a balance between hydrophilic and hydrophobic parameters is important in drug discovery. Therefore, we calculated water solubility (mg/L). Poorly soluble drugs require high doses in order to reach therapeutic effect. Water solubility data computed *via* Pre-ADMET indicated that only compound **4e** (16.26 mg/L) and reference drug diazepam (6.17 mg/L) have shown good solubility compared to others (Table 3). Human Intestinal Absorption (HIA) computed by using AdmetSAR online software revealed that all the compounds have 97–100% absorption range. Another drug-like attribute in drug discovery is low plasma protein binding (PPB). It is assumed that unbound drugs are available to interact with their pharmacological target receptors. Plasma protein binding percentage of the synthesized drugs was computed using Pre-ADMET online server (Table 3). The data in Table 3 revealed that the PPB of compounds have high PPB ranging from 89.0 to 95.7%. It means that 4.3–11% of the drug in the plasma is unbound. It is reported in literature that 45% of the newly approved drugs have > 95% PPB and 24% are > 99% [38]. Hence, according to free drug hypothesis, compound **4e** with 11% unbound drug is available for pharmacological interaction. This is in confirmation with *in-vivo* results. Only **4e** displayed anticonvulsive potential at the dose of 10 mg/kg and 30 mg/kg (Table 2).

To target central nervous system, blood brain barrier (BBB) penetration is vital for antiepileptic drug design. We have computed BBB penetration using two online servers. Pre-ADMET server compute BBB penetration as [brain]/[blood]. According to the Pre-ADMET classification, for high CNS absorption the value should be > 2.0. While, moderate and low permeable cross BBB with the value of 2.0–0.1 and < 0.1 respectively. The computed values are listed in Table 3. It can be concluded from Table 3 values that compounds **4a**, **4e–h** have moderate ability to cross BBB. The red highlighted compounds **4b–d** have poor crossing efficiency. The data also showed that reference drug diazepam has high BBB crossing potential. Further, we also used online BBB predictor from AlzPlatform (www.cbligand.org/AD/) [39]. All compounds except **4a** and **4f** showed moderate ability to cross BBB. Finally, toxicity/carcinogenicity of the compounds was calculate using AdmetSAR online server (lmmd.ecust.edu.cn/admetsar1/). Only compound **4c** showed AMES toxicity. All the other compounds are predicted as safe. Predicted BBB scores of synthesized compounds (**4a–i**) using online BBB predictor from AlzPlatform are presented in Fig. S3-S-4 in Supporting Information.

3. Conclusions

Since last decade, the drug discovery paradigm has been shifted to multitarget designed ligands (polyvalent) in which a single chemical entity may be able to hit multiple targets simultaneously. Based on this

shift, the main aim of our current study was to identify a drug or molecule which at one hand can target the excitability of the brain to exert its calm effect and on other hand proportionally decrease excitotoxicity to prevent the progression of Alzhiemer disease. In this study, a series of carboxamide analogs have been synthesized *via* Suzuki cross-coupling reaction. The compounds **(4a–4i)** were obtained in moderate to good yields. The reaction conditions were found suitable for different electron donating and withdrawing moieties. The synthesized compounds showed good inhibitory activity against cholinesterases. Some compounds showed selectivity for BChE. Overall, a number of compounds showed IC_{50} value in low micromolar level. Furthermore, *in-vivo* screening of synthesized carboxamide derivatives for identification of their potential against seizure was also carried out. Only compounds **4e** and **4h** were able to show some anticonvulsant potential. Binding affinity data computed *via* docking simulations against GABA-A/GABA-AT receptors showed that these receptors are possible mechanism of action for the synthesized compounds. We were in opinion that the lack of drug activity may be due poor pharmacokinetic parameters, therefore, we proceeded towards calculation of pharmacological and pharmacokinetic parameters. Our *in-silico* predictions suggest that the plasma protein binding, low to moderate blood brain barrier penetration and low solubility are the main attributes of low *in-vivo* performance.

4. Material and methods

4.1. General Information

Melting points are uncorrected. ^{1}H, ^{13}C-NMR spectra were obtained in $CDCl_3$ (400/100 MHz) (Bruker, MA, USA), respectively. EI-MS spectra were obtained on a JMS-HX-110 spectrometer (JEOL, MA, USA). For column chromatography, silica gel (70–230 mesh) was used. The reactions were monitored on TLC cards (Merck silica gel 60 PF_{254}). UV lamp (254–365 nm) was used for visualization of compounds. Final products were for their purity on Schimadzu system using C18 column and isocratic solvent system of water/acetonitrile 50:50) at room temperature. For elemental analyses CHN Perkin-Elmer 2400 series analyzer was used.

4.2. General procedure for the synthesis of intermediate 5-bromo-N-(4-methylpyridin-2-yl)thiophene-2-carboxamide (3)

$TiCl_4$ (43.5 mmol, 3.0 eq, 4.78 mL) and the 2-amino-4-methylpyridine (**1**, 14.48 mmol, 1 eq, 3 g) were added to a solution of 5-bromothiophene-2-carboxylic acid (**2,** 14.48 mmol, 1 eq, 1.567 g) in pyridine (150 mL). The sealed Schlenk flask containing the reaction mixture was stirred for 2 h at 85 °C. After cooling reaction mixture, and after removing pyridine by co-evaporation with toluene, was treated with an aq. solution of 1 N HCl (150 mL) and extracted with dichloromethane (3 × 150 mL). The washing of combined organic layers was done with saturated aq. solution of sodium bicarbonate (3 × 150 mL), dried over sodium sulfate anhydrous and evaporated to dryness under reduced pressure. The obtained crude product was further purified by column chromatography using 10% solution of *n*-hexane, ethyl acetate.

4.3. General procedure for Suzuki coupling of amide

The catalyst $Pd(PPh_3)_4$ (7 mol%, 0.0544 g) was added in intermediate compound (**3**,1 eq, 0.673 mmol, 0.2 g), under nitrogen atmosphere. The 1,4-dioxane was added (8 mL) and stirring of the reaction mixture was done for 30 min. The boronic acid (1.1 eq, 0.741 mmol), K_3PO_4 (2 eq, 1.35 mmol, 0.284 g) and water (2 mL) were added [33,34]. The reaction mixture was stirred for 20–25 h at 90 °C. Then it was cooled to room temperature (rt), and diluted with ethyl acetate. After separation of organic layer $MgSO_4$ was added for drying and then the solvent was removed under vacuum. The crude residue was purified by column chromatography by using *n*-hexane and ethyl acetate (25%).

4.3.1. 5-Bromo-N-(4-methylpyridin-2-yl)thiophene-2-carboxamide (3)

White porous solid, mp = 105–106 °C, (80% 3.44 g), ^{1}H NMR (400 MHz, $CDCl_3$) δ 8.92 (s, 1H), 8.15 (d, J = 8.0 Hz, 2H), 7.46 (d, J = 4.0 Hz, 1H), 7.10 (d, J = 4.0 Hz, 1H), 6.93 (d, J = 4.0 Hz, 1H), 2.41 (s, 3H). ^{13}C NMR (100 MHz, $CDCl_3$) δ 159.0, 151.1, 150.6, 147.0, 140.5, 130.9, 128.8, 121.4, 119.8, 115.2, 21.5. EI/MS *m/z* (%): 298.0 $[M+H]^+$, 299.2 [M + 2]; [M-CH_3] = 281.3; [M-Br] = 217.4. Anal. Calcd. For $C_{11}H_9BrN_2OS$: C, 44.46; H, 3.05; N, 9.43. Found: C, 44.40; H, 3.03; N, 9.40%.

4.3.2. 5-(3-Chlorophenyl)-N-(4-methylpyridin-2-yl)thiophene-2-carboxamide (4a)

Off white solid, mp = 154–156 °C, (84%, 180 mg), ^{1}H NMR (400 MHz, $CDCl_3$) δ 8.94 (s, 1H), 8.10 (s, 1H), 8.05 (d, J = 4.1 Hz, 1H), 7.54–7.51 (m, 3H), 7.40–7.39 (m, 3H), 6.87 (d, J = 5.1 Hz, 1H), 2.50 (s, 3H). ^{13}C NMR (100 MHz, $CDCl_3$) δ 165.4, 159.1, 152.9, 150.4, 144.4, 139.9, 131.3, 129.8, 126.4, 125.5, 123.6, 121.2, 120.6, 115.4, 22.6. EI/MS *m/z* (%): 329.9 $[M+H]^+$; [M-Cl] = 293.1; [M-Cl, CH_3] = 278.0. Analysis calculated for $C_{17}H_{13}ClN_2OS$: C, 62.10; H, 3.98. N, 8.52. Found: C, 62.04; H, 3.97; N, 8.55%. HPLC purity = 100.0%. T_R = 22.2 min.

4.3.3. Methyl 4-(5-((4-methylpyridin-2-yl)carbamoyl)thiophen-2-yl) benzoate (4b)

off white solid, mp = 199–200 °C, (35%, 83 mg), ^{1}H NMR (400 MHz, $CDCl_3$) δ 9.51 (s, 1H), 8.26 (s, 1H), 8.18–8.06 (m, 3H), 7.86 (d, J = 4.0 Hz, 1H), 7.72–7.70 (m, 2H), 7.43 (d, J = 4.0 Hz, 1H), 6.94 (d, J = 8 Hz, 1H), 3.95 (s, 3H), 2.42 (s, 3H). ^{13}C NMR (100 MHz, $CDCl_3$) δ 164.3, 162.2, 159.0, 158.0, 147.0, 142.1, 139.0, 138.7, 136.8, 131.2, 129.0, 128.0, 127.8, 126.0, 125.4, 120.0, 111.8, 51.0, 21.6. EI/MS *m/z* (%): 353.5 $[M+H]^+$; [M-CH_3] = 337.3; [M-$COOCH_3$] = 293.4. Anal. Calcd. For $C_{19}H_{16}N_2O_3S$: C, 64.76; H, 4.58; N, 7.95. Found: C, 64.70; H, 4.56; N, 7.97%. HPLC purity = 98.3%. T_R = 15.3 min.

4.3.4. 5-(4-Methoxyphenyl)-N-(4-methylpyridin-2-yl)thiophene-2-carboxamide (4c)

Light yellow solid, mp = 145–147 °C, (84%, 183 mg), ^{1}H NMR (400 MHz, $CDCl_3$) δ 8.84 (s, 1H), 8.20 (s, 1H), 8.12 (d, J = 4.0 Hz, 1H), 7.63 (d, J = 3.9 Hz, 1H), 7.57–7.54 (m, 2H), 7.18 (d, J = 3.9 Hz, 1H), 6.95–6.91 (m, 2H), 6.88 (d, J = 4.4 Hz, 1H), 3.84 (s, 3H), 2.39 (s, 3H). ^{13}C NMR (100 MHz, $CDCl_3$) δ 162.1, 160.1, 158.0, 157.1, 147.1, 143.0, 139.0, 138.2, 129.1, 127.5, 126.1, 125.2, 121.0, 115.0, 114.0, 111.0, 56.0, 22.0. EI/MS *m/z* (%): 325.1 $[M+H]^+$; [M-OCH_3] = 293.3; [M-CH_3, $-OCH_3$] = 278.4. Anal. Calcd. For C18H16N2O2S: C, 66.65; H, 4.97; N, 8.64. Found: C, 66.60; H, 4.99; N, 8.66%. HPLC purity = 99.4%. T_R = 14.9 min.

4.3.5. N-(4-methylpyridin-2-yl)-5-(4-(methylthio)phenyl)thiophene-2-carboxamide (4d)

off white solid, mp = 167–169 °C, (71%, 162 mg), ^{1}H NMR (400 MHz, $CDCl_3$) δ 8.88 (s, 1H), 8.20 (s, 1H), 8.12 (d, J = 5.1 Hz, 1H), 7.65 (d, J = 3.9 Hz, 1H), 7.55 (d, J = 8.3 Hz, 2H), 7.28–7.25 (m, 3H), 6.89 (d, J = 5.0 Hz, 1H), 2.51 (s, 3H), 2.39 (s, 3H). ^{13}C NMR (100 MHz, $CDCl_3$) δ 162.0, 160.1, 158.0, 147.4, 141.0, 138.0, 137.0, 136.7, 131.0, 129.0, 128.7, 127.4, 126.0, 125.0, 122.8, 111.0, 22.0, 15.6. EI/MS *m/z* (%): 341.1 $[M+H]^+$; [M-CH_3] = 325.3; [M-CH_3,-SCH_3] = 278.3. Anal. Calcd. For $C_{18}H_{16}N_2OS_2$: C, 63.50; H, 4.74; N, 8.23. Found: C, 63.53; H, 4.72; N, 8.20%. HPLC purity = 98.0%. T_R = 19.2 min.

4.3.6. 5′-Methyl-N-(4-methylpyridin-2-yl)-[2,2′-bithiophene]-5-carboxamide (4e)

Light brown solid, mp = 134–136 °C, (80%, 168 mg), ^{1}H NMR (400 MHz, $CDCl_3$) δ 8.96 (s, 1H), 8.20 (s, 1H), 8.16–8.11 (m, 2H), 7.59

(d, J = 3.8 Hz, 1H), 7.11–7.06 (m, 1H), 6.90 (s, 1H), 6.72 (d, J = 2.3 Hz, 1H), 2.51 (s, 3H), 2.40 (s, 3H). ^{13}C NMR (100 MHz, $CDCl_3$) δ 165.4, 159.8, 151.2, 148.4, 144.7, 138.1, 137.1, 135.4, 131.2, 128.4, 127.9, 125.0, 117.2, 115.1, 22.5. EI/MS m/z (%): 315.6 $[M+H]^+$; [M-CH_3] = 299.1; [M-2CH_3] = 284.0. Anal. Calcd. For $C_{16}H_{14}N_2OS_2$: C, 61.12; H, 4.49; N, 8.91. Found: C, 61.19; H, 4.50; N, 8.79%. HPLC purity = 99.6%. T_R = 16.3 min.

4.3.7. 5-(3,4-dichlorophenyl)-N-(4-methylpyridin-2-yl)thiophene-2-carboxamide (4f)

White crystalline solid, mp = 178–180 °C, (83%, 202 mg), ^{1}H NMR (400 MHz, $CDCl_3$) δ 8.91 (s, 1H), 8.21 (s, 1H), 8.15 (d, J = 4.9 Hz, 1H), 7.73 (s, 1H), 7.68 (d, J = 3.5 Hz, 1H), 7.48 (q, J = 8.4 Hz, 2H), 7.31 (d, J = 3.5 Hz, 1H), 6.94 (d, J = 4.5 Hz, 1H), 2.43 (s, 3H). ^{13}C NMR (100 MHz, $CDCl_3$) δ 165.4, 161.1, 159.8, 150.5, 148.4, 144.4, 137.8, 130.7, 128.4, 126.1, 124.6, 122.1, 121.1, 117.4, 117.2, 115.4, 21.9. EI/MS m/z (%): 364.0 $[M+H]^+$, 365.2 [M+2]; 367.3 [M+4]; [M-2Cl] = 292.1; Anal. Calcd. For $C_{17}H_{12}C_{l2}N_2OS$: C, 56.21; H, 3.33; N, 7.71. Found: C, 56.14; H, 3.35; N, 7.70%. HPLC purity = 96.9%. T_R = 21.3 min.

4.3.8. 5-(3-chloro-4-fluorophenyl)-N-(4-methylpyridin-2-yl)thiophene-2-carboxamide (4g)

white porous solid, mp = 188–190 °C, (74%, 172 mg), ^{1}H NMR (400 MHz, $CDCl_3$) δ 8.91 (s, 1H), 8.22 (s, 1H), 8.15 (d, J = 5.1 Hz, 1H), 7.69 (m, 2H), 7.53–7.49 (m, 1H), 7.29 (m, 1H), 7.21 (t, J = 8.6 Hz, 1H), 6.94 (d, J = 4.8 Hz, 1H), 2.43 (s, 3H). ^{13}C NMR (100 MHz, $CDCl_3$) δ 159.7 (d, J = 20 Hz), 157.1, 152.8, 150.5, 148.4, 144.4, 137.9, 130.6 (d, J = 5 Hz), 128.4, 126.1(d, J = 7 Hz), 124.6, 122.0 (d, J = 19 Hz), 121.07, 117.4, 117.2, 115.3, 21.9 EI/MS m/z (%): 347.0 $[M+H]^+$, 348.0 [M+2]; [M-Cl] = 311.0. Anal. Calcd. For $C_{17}H_{12}ClFN_2OS$: C, 58.88; H, 3.49; N, 8.08. Found: C, 58.85; H, 3.51; N, 8.06%. HPLC purity = 95.9%. T_R = 18.0 min.

4.3.9. 5-(4-chlorophenyl)-N-(4-methylpyridin-2-yl)thiophene-2-carboxamide (4h)

Off white solid, mp = 190–191 °C, (75%, 166 mg), ^{1}H NMR (400 MHz, $CDCl_3$) δ 8.89 (s, 1H), 8.19 (s, 1H), 8.12 (d, J = 5.1 Hz, 1H), 7.65 (d, J = 3.9 Hz, 1H), 7.57–7.54 (m, 2H), 7.39–7.36 (m, 2H), 7.27 (d, J = 4.0 Hz, 1H), 6.90 (d, J = 5.1 Hz, 1H), 2.40 (s, 3H). ^{13}C NMR (100 MHz, $CDCl_3$) δ 162.0, 160.1, 158.3, 146.1, 142.2, 140.1, 138.2, 135.0, 132.2, 131.0, 129.1, 127.1, 126.3, 124.1, 121.0, 112.3, 21.9. EI/MS m/z (%): 329.9 $[M+H]^+$; [M-Cl] = 293.1; [M-Cl, CH_3] = 278.0; [M-Cl, Aryl fragment] = 217.2. Anal. Calcd. For $C_{17}H_{13}ClN_2OS$: C, 62.10; H, 3.99; N, 8.52. Found: C, 62.04; H, 3.97; N, 8.56%. HPLC purity = 998.1%. T_R = 20.4 min.

4.3.10. 5-(3-acetylphenyl)-N-(4-methylpyridin-2-yl)thiophene-2-carboxamide (4i)

Light brown solid, mp = 164–166 °C, (53% 120 mg), ^{1}H NMR (400 MHz, $CDCl_3$) δ 8.78 (s, 1H), 8.24 (d, J = 7.0 Hz, 2H), 8.17 (d, J = 5.0 Hz, 1H), 7.96 (d, J = 7.7 Hz, 1H), 7.85 (d, J = 7.7 Hz, 1H), 7.71 (d, J = 3.8 Hz, 1H), 7.56 (t, J = 7.7 Hz, 1H), 7.42 (d, J = 3.9 Hz, 1H), 6.95 (d, J = 4.7 Hz, 1H), 2.68 (s, 3H), 2.44 (s, 3H). ^{13}C NMR (100 MHz, $CDCl_3$) δ 198.0, 162.0, 158.0, 157.9, 147.0, 143.9, 139.0, 137.0, 136.0, 134.0, 130.2, 129.0, 128.2, 127.0, 125.9, 122.2, 111.3, 27.0, 22.5. EI/MS m/z (%): 337.5 $[M+H]^+$; [M-$COCH_3$] = 293.3; [M-CH_3, −$COCH_3$] = 278.3. Anal. Calcd. For $C_{19}H_{16}N_2O_2S$: C, 67.84; H, 4.79; N, 8.33. Found: C, 67.89; H, 4.77; N, 8.30%. HPLC purity = 97.8.0%. T_R = 17.5 min.

4.4. Pharmacology

4.4.1. In-vitro inhibition of cholinesterases

In-vitro inhibition of cholinesterases were carried out by following procedures already reported by our research group [23,24]. By using μQuant microplate spectrophotometer (MQX200, BioTek USA) all the synthesized compounds evaluated for their AChE (Electrophorous electricus type-VI-S, Sigma-Aldrich GmbH 4USA, code 1001596210) and BChE inhibition (Equine serum Lyophilized Sigma-Aldrich GmbH USA, code 101292670). Stock solution of the test derivatives were prepared by using DMSO (I mL) and 0.1 M phosphate buffer (KH_2PO_4/K_2HPO_4) of pH 8.0 (9 mL). Appropriate quantity of DTNB (Ellman's reagent), synthesized compounds, 0.03 U/ml of enzymes (AChE and BChE) were reacted by pre-incubating at 30 °C for 10 min and after addition of 1 mM ATCI or BTCI further incubation was done for 15 min. The enzymatic hydrolysis was measured at 412 nm using μQuant microplate spectrophotometer (MQX200, BioTek USA). DMSO was used as negative control. Each reading was taken in triplicate and the IC_{50} values were obtained by plotting sample conc. vs inhibition.

4.4.2. Animals and experimental procedure

BALB/c mice (7–8 weeks old) of either sex weighing 25 ± 3 g were obtained from National Institute of Health animal breeding facility, Islamabad. These animals were allowed to acclimatize for minimum period of 1 week in the animal house facility of Department of Pharmacology, Bahauddin Zakariya University, Multan to get familiarize with the new environment. Six mice were accommodated in each transparent polycarbonate cage having floor area of 750 cm^2 with environmental enrichment and under controlled temperature (22–25 °C and humidity (45–55%) with 12 h light and dark cycle. They had free access to food (Crystal Feed Industry, Multan; Protein 22% and Carbohydrate 60%) and water ad libitum. The sawdust bedding from Eastern white pine wood in the polycarbonate cages were routinely changed every 5 days and animals were monitored for their wellbeing on daily basis. In total 10 groups each having 6–8 mice were made for the evaluation of anticonvulsive potential of standard and experimental drugs. Group 1 served as seizure control group and treated with chemoconvulsive agent i.e. pentylenetetrazole (PTZ 90 mg/kg, i.p.), group 2 was the standard group and administered diazepam 5 mg/kg (i.p.), groups 3–10 were initially treated with the test compounds **4a–4i** at the dose of 10 mg/kg to screen any anticonvulsive potential. For those compounds which demonstrated anti-seizure potential, the dose was further increased to 30 mg/kg. All the test compounds were suspended in Tween 80 and water mixture (5% W/V) and administered by the oral gavage 30–40 min before challenging with 90 mg/kg of pentylenetetrazole (dissolved in normal saline) [40–43]. These mice were observed for 30 min after challenging with PTZ with the consideration of following parameters;

1) Latency to onset of first myoclonic jerks
2) Latency to onset of Generalized clonic convulsions
3) % age of animals showed convulsions
4) % age of animals protected from convulsions

Ideally, no sign of severe illness should appear after PTZ challenge with the exception of convulsions. All the experiments on animals were performed in compliance with the ARRIVE guidelines. Care was exercised for minimal number of animal usage as defined by the principle of 3Rs, i.e., Replacement, Reduction and refinement. The Bahauddin Zakariya University Multan ethical committee has further endorsed the protocol *via* Notification Number EC/BZU/197 dated 18 May 2018. According to protocol all survived animals after experimental trials were euthanized by administration of 75 mg/kg of Pentobarbital to minimize the suffering and pain.

4.4.2.1. Statistical analysis. Data values are represented as mean ± SEM (standard error of the mean) (n = 6–8). Statistical analysis was performed by using one-way Analysis of variance (ANOVA) followed by Dunnett's test.

4.5. In-silico studies

4.5.1. Docking studies

Docking simulations were performed using Molecular Operating Environment (MOE 2016:0802) package [44]. Three-dimensional crystal structures of the targets were downloaded from Protein Data Bank. Structure of human GABA-A receptor (PDB accession code = 4COF) complexed with benzamidine as native ligand. While, a pentameric ligand-gated ion-channel from Erwinia chrysanthemi (PDB accession code 2YOE). The downloaded enzymes were prepared according to our previously reported parameters [24,45]. The structures of the compounds were drawn by using molecular builder option of MOE. The ligands were energy minimized using MMFF94 forcefield. All these compounds were docked into the binding sites of the prepared enzymes. Default docking parameters were set and ten different conformations were generated for each compound. Lowest binding energy ligand enzyme complexes were visualized by MOE ligand interaction module. While for 3-D interaction plot, discovery studio visualizer was used [46].

4.5.2. In-silico pharmacokinetic predictions

For the prediction of in-silico pharmacokinetics of the synthesized compounds, MOE and different online servers were used. Lipinski descriptors were calculated from database viewer (.mdb) file. For AdmetSAR server, Simplified Molecular Input Line Entry Specification (SMILES), representing a 2D chemical drawing as a string, was generated from 2D structural models and used as input. MOL file format was used to calculate the ADME properties from online Pre-ADMET and BBB predictor server.

Funding

The research was funded by Higher Education Commission (HEC), Pakistan.

Declaration of Competing Interest

All authors declare that they have no conflict of interest.

Acknowledgements

This work is a part of the Ph.D. research of Mr. Gulraiz Ahmad. Dr. Umer Rashid has purchased MOE 2016.08 license under Higher Education Commission, Pakistan, project No. 5291/Federal/NRPU/R&D/HEC/2016.

Appendix A. Supplementary material

Supplementary data to this article can be found online at https://doi.org/10.1016/j.bioorg.2019.103216.

References

[1] M. Manford, Recent advances in epilepsy, J. Neurol. 264 (8) (2017) 1811–1814.
[2] C.E. Stafstrom, L. Carmant, Seizures and epilepsy: an overview for neuroscientists, Cold Spring Harb. Perspect. Med. 5 (2015) a022426.
[3] S. Suruchi, D. Vaishali, Epilepsy–a comprehensive review, Int. J. Pharm. Res. Rev. 2 (12) (2013) 61–80.
[4] A. Sen, V. Capelli, M. Husain, Cognition and dementia in older patients with epilepsy, Brain 141 (6) (2018) 1592–1608.
[5] M. Bialer, Chemical properties of antiepileptic drugs (AEDs), Adv. Drug. Deliv. Rev. 64 (2012) 887–895.
[6] R. Sankaraneni, D. Lachhwani, Antiepileptic drugs-a review, Pediatr Ann. 44 (2) (2015) 36–42.
[7] F. Salia, T.F. Pouya, K.R. Eva, J.L. John, A.M. Marek, Antiepileptic drugs in critically ill patients, Critic. Care 22 (1) (2018) 153.
[8] U. Rashid, F.L. Ansari, Challenges in designing therapeutic agents treating Alzheimer ‘s disease-form serendipity to rationality, Drug Design Discovery in Alzheimer ‘s Disease, Elsevier, 2014, pp. 40–141.
[9] D. Friedman, L.S. Honig, N. Scarmeas, Seizures and epilepsy in Alzheimer's disease, CNS. Neurosci. Ther. 18 (2012) 285–294.
[10] A. Horváth, A. Szűcs, G. Barcs, J.L. Noebels, A. Kamondi, Epileptic seizures in alzheimer disease, a review, Alzheimer Dis. Assoc. Disord. 30 (2) (2016) 186–192.
[11] F.S. Giorgi, M. Guida, A. Vergallo, U. Bonuccelli, G. Zaccara, Treatment of epilepsy in patients with Alzheimer's disease, Expert Rev. Neurother. 17 (3) (2017) 309–318.
[12] F. Raudino, Alzheimers’ disease and epilepsy: a literature review, Arch. Neurosci. 4 (2) (2017) 39578.
[13] K.A. Vossel, A.J. Beagle, G.D. Rabinovici, H. Shu, S.E. Lee, G. Naasan, M. Hegde, S.B. Cornes, M.L. Henry, A.B. Nelson, W.W. Seeley, M.D. Geschwind, M.L. Gorno-Tempini, T. Shih, H.E. Kirsch, P.A. Garcia, B.L. Miller, L. Mucke, Seizures and epileptiform activity in the early stages of Alzheimer disease, JAMA Neurol. 70 (9) (2013) 1158–1166.
[14] J.H. Jeong, B.Y. Choi, A.R. Kho, S.H. Lee, D.K. Hong, S.H. Lee, S.Y. Lee, H.K. Song, H.C. Choi, S.W. Suh, Diverse effects of an acetylcholinesterase inhibitor, donepezil, on hippocampal neuronal death after pilocarpine-induced seizure, Int. J. Mol. Sci. 18 (11) (2017) 2311.
[15] A. Mishra, R.K. Goel, Adjuvant anticholinesterase therapy for the management of epilepsy-induced memory deficit: a critical pre-clinical study, Basic Clin. Pharmacol. Toxicol. 115 (6) (2014) 512–517.
[16] P. Mares, A. Mikulecka, Different effects of two N-methyl-D-aspartate receptor antagonists on seizures, spontaneous behavior, and motor performance in immature rats, Epilepsy Behav. 14 (1) (2009) 32–39.
[17] A. Dhir, K. Chopra, Memantine delayed N-methyl-D-aspartate -induced convulsions in neonatal rats, Fundam. Clin. Pharmacol. 29 (1) (2015) 72–78.
[18] A. Bakker, G.L. Krauss, M.S. Albert, C.L. Speck, L.R. Jones, C.E. Stark, M.A. Yassa, S.S. Bassett, A.L. Shelton, M. Gallagher, Reduction of hippocampal hyperactivity improves cognition in amnestic mild cognitive impairment, Neuron 74 (3) (2012) 467–474.
[19] P. Feliciano, Antiepileptic drugs in Alzheimer’s, Nat. Genet. 44 (9) (2012) 967 967.
[20] C.S. Musaeus, M.M. Shafi, E. Santarnecchi, S.T. Herman, D.Z. Press, Levetiracetam Alters Oscillatory Connectivity in Alzheimer's Disease, J. Alzheimers Dis. 58 (4) (2017) 1065–1076.
[21] P.E. Sanchez, L. Zhu, L. Verret, K.A. Vossel, A.G. Orr, J.R. Cirrito, N. Devidze, K. Ho, G.Q. Yu, J.J. Palop, L. Mucke, Levetiracetam suppresses neuronal network dysfunction and reverses synaptic and cognitive deficits in an Alzheimer's disease model, Proc. Natl. Acad. Sci. USA 109 (2012) 2895–2903.
[22] H.B. Nygaard, A.C. Kaufman, T. Sekine-Konno, L.L. Huh, H. Going, S.J. Feldman, M.A. Kostylev, S.M. Strittmatter, Brivaracetam, but not ethosuximide, reverses memory impairments in an Alzheimer's disease mouse model, Alzheimers Res. Ther. 7 (1) (2015) 25.
[23] S. Ahmad, F. Iftikhar, F. Ullah, A. Sadiq, U. Rashid, Rational design and synthesis of dihydropyrimidine based dual binding site acetylcholinesterase inhibitors, Bioorg. Chem. 69 (2016) 91–101.
[24] S.T. Tanoli, M. Ramzan, A. Hassan, A. Sadiq, M.S. Jan, F.A. Khan, F. Ullah, H. Ahmad, M. Bibi, T. Mahmood, U. Rashid, Design, synthesis and bioevaluation of tricyclic fused ring system as dual binding site acetylcholinesterase inhibitors, Bioorg. Chem. 83 (2019) 336–347.
[25] K. Rizwan, N. Rasool, R. Rehman, T. Mahmood, K. Ayub, T. Rasheed, G. Ahmad, A. Malik, S.A. Khan, M.N. Akhtar, N.B. Alitheen, M.N.M. Aziz, Facile synthesis of N-(4-bromophenyl)-1- (3-bromothiophen-2-yl)methanimine derivatives *via* Suzuki cross-coupling reaction, their characterization and DFT studies, Chem. Cent. J. 12 (2018) 84.
[26] K. Rizwan, M. Zubair, N. Rasool, T. Mahmood, K. Ayub, N.B. Alitheen, M.N.M. Aziz, M.N. Akhtar, F.H. Nasim, S.M. Bukhary, V.U. Ahmad, M. Rani, Palladium (0) catalyzed Suzuki cross-coupling reaction of 2, 5-dibromo-3-methylthiophene selectivity, characterization, DFT studies and their biological evaluations, Chem. Cent. J. 12 (2018) 49.
[27] H.M. Ikram, N. Rasool, G. Ahmad, G.A. Chotana, S.G. Musharraf, M. Zubair, M. zia-ul-Haq, H.Z. Jaafar, Selective C-Arylation of 2, 5-Dibromo-3-hexylthiophene via Suzuki cross coupling reaction and their pharmacological aspects, Molecules 20 (2015) 5202–5214.
[28] H.M. Ikram, N. Rasool, M. Zubair, K.M. Khan, G.A. Chotana, M.N. Akhtar, N. Abu, N.B. Alitheen, A.M. Elgorban, U.A. Rana, Efficient double suzuki cross-coupling reactions of 2, 5-dibromo-3-hexylthiophene anti-tumor, haemolytic, anti-thrombolytic and biofilm inhibition studies, Molecules 21 (2016) 977.
[29] T. Rasheed, N. Rasool, M. Noreen, Y. Gull, M. Zubair, A. Ullah, U.A. Rana, Palladium (0) catalyzed Suzuki cross-coupling reactions of 2,4-dibromothiophene: selectivity, characterization and biological applications, J. Sulfur Chem. 36 (2015) 240–250.
[30] A. Asadipour, M. Alipour, M. Jafari, M. Khoobi, S. Emami, H. Nadri, A. Sakhteman, A. Moradi, V. Sheibani, F. Homayouni Moghadam, A. Shafiee, A. Foroumadi, Novel coumarin-3-carboxamides bearing N-benzylpiperidine moiety as potent acetylcholinesterase inhibitors, Eur. J. Med. Chem. 70 (2013) 623–630.
[31] J. Gierbolini, M. Giarratano, S.R. Benbadis, Carbamazepine-related antiepileptic drugs for the treatment of epilepsy-a comparative review, Expert. Opin. Pharmacother. 17 (2016) 885–888.
[32] Y. Xu, J.P. Colletier, M. Weik, H. Jiang, J. Moult, I. Silman, J.L. Sussman, Flexibility of aromatic residues in the active-site gorge of acetylcholinesterase X-ray versus molecular dynamics, Biophys. J. 95 (2008) 2500–2511.
[33] G. Kryger, I. Silman, J.L. Sussman, Structure of acetylcholinesterase complexed with E2020 (Aricept): implications for the design of new anti-Alzheimer drugs, Structure 7 (3) (1999) 297–307.
[34] Y. Nicolet, O. Lockridge, P. Masson, J.C. Fontecilla-Camps, F. Nachon, Crystal structure of human butyrylcholinesterase and of its complexes with substrate and products, J. Biol. Chem. 278 (2003) 41141–41147.

[35] M. Bajda, A. Wieckowska, M. Hebda, N. Guzior, C.A. Sotriffer, B. Malawska, Structure-based search for new inhibitors of cholinesterases, Int. J. Mol. Sci. 14 (2013) 5608–5632.
[36] A. Rahman, M.T. Ali, M.M. Shawan, M.G. Sarwar, M.A. Khan, M.A. Halim, Halogen-directed drug design for Alzheimer's disease: a combined density functional and molecular docking study, Springer Plus 5 (2016) 1346.
[37] P.S. Miller, A.R. Aricescu, crystal structure of a human $GABA_A$ receptor, Nature 512 (2014) 270.
[38] X. Liu, M. Wright, C.E. Hop, Rational use of plasma protein and tissue binding data in drug design, J. Med. Chem. 57 (2014) 8238–8248.
[39] L. Haibin, W. Lirong, L. Mingliang, P. Rongrong, L. Peibo, P. Zhong, W. Yonggang, S. Weiwei, X. Xiang-Qun, AlzPlatform. An Alzheimer's Disease domain-specific chemogenomics knowledgebase for polypharmacology and target identification research, J. Chem. Inf. Model. 54 (2014) 1050–1060.
[40] D.M. Abdallah, Anticonvulsant potential of the peroxisome proliferator-activated receptor gamma agonist pioglitazone in pentylenetetrazole-induced acute seizures and kindling in mice, Brain Res. 1351 (2010) 246–253.
[41] İ. Kaputlu, T. Uzbay, L-NAME inhibits pentylenetetrazole and strychnine-induced seizures in mice, Brain Res. 753 (1997) 98–101.
[42] A.V. Zaitsev, K.K. Kim, D.S. Vasilev, N.Y. Lukomskaya, V.V. Lavrentyeva, N.L. Tumanova, I.A. Zhuravin, L.G. Magazanik, N-methyl-D-aspartate receptor channel blockers prevent pentylenetetrazole induced convulsions and morphological changes in rat brain neurons, J. Neurosci. Res. 93 (2015) 454–465.
[43] L.R. Vilela, D.C. Medeiros, G.H. Rezende, A.C. de Oliveira, M.F. Moraes, F.A. Moreira, Effects of cannabinoids and endocannabinoid hydrolysis inhibition on pentylenetetrazole-induced seizure and electroencephalographic activity in rats, Epilepsy Res. 104 (2013) 195–202.
[44] Molecular Operating Environment (MOE), 2016.08; Chemical Computing Group ULC, 1010 Sherbooke St. West, Suite #910, Montreal, QC, Canada, H3A 2R7, 2018.
[45] F. Iftikhar, F. Yaqoob, N. Tabassum, M.S. Jan, A. Sadiq, S. Tahir, T. Batool, B. Niaz, F.L. Ansari, M.I. Choudhary, Design, synthesis, in-vitro thymidine phosphorylase inhibition, in-vivo antiangiogenic and in-silico studies of C-6 substituted dihydropyrimidines, Bioorg. Chem. 80 (2018) 99–111.
[46] Dassault Systèmes BIOVIA, Discovery Studio Modelling Environment, Release 4.5, San Diego: Dassault Systems, 2015.